



Subcellular localization of GLUT1 in the acini and striated ducts of the sublingual major salivary glands in female rats (immunohistochemical study)

Maha El Shahawy^{1,2*}, Menna Abdulqader El-Badawy³

¹Associate Professor, Oral Biology Department, Faculty of Dentistry, Minia University, Minia 51161, Egypt

²Associate Professor, Oral Biology Department, Faculty of Dentistry, Kafrelsheikh University, Elgiesh street, Kafrelsheikh 33516, Egypt

maha.elshahawy@minia.edu.eg ORCID ID: [0000-0001-7122-1191](https://orcid.org/0000-0001-7122-1191)

³Demonstrator at Department of Oral Biology, Faculty of Dentistry, Assiut University, Assiut, 71515, Egypt. Faculty of Dentistry, Assiut University, Assiut 71515, Egypt.

menna_abdulqader@dent.aun.edu.eg ORCID: [0009-0000-4680-4491](https://orcid.org/0009-0000-4680-4491)

* Corresponding author: maha.elshahawy@minia.edu.eg

Received 30 April 2024; revised 06 July 2024; accepted 5 November 2024

Abstract

Background: Sublingual salivary gland (SLGs) is one of the major salivary glands that is predominantly mucous in nature. The glucose transporter 1 (GLUT1) is responsible for the transport of monosaccharides and is localized in the parotid and submandibular major salivary glands, however GLUT1 localization in the SLGs is hitherto unknown. **Objective:** To investigate the distribution patterns of GLUT1 in adult female SLG's lobular structures of the control female rats. **Material and method:** The SLGs were assessed by hematoxylin and eosin (H&E) and Masson trichrome. The GLUT1 immunohistochemistry was utilized to localize the protein in the SLG tissue, followed by histomorphometric analysis of the GLUT1 immunoreaction's optical intensity. **Results:** The SLG tissue revealed GLUT1 localization in the mucous acini and in the striated ducts (SDs). Histomorphometric analysis revealed a lesser intensity of GLUT1 immunoreaction in the acini in comparison to the SDs ($P=0.000$) **Conclusion:** GLUT1+ immunolabelling was depicted in the acini and the SDs of the SLGs, however the optical intensity of the GLUT1 immunolabelling was significantly higher in the SDs than the acini, which may reflect a higher energy requirement in the SDs. Based on the localization of GLUT1 in the SLG, new treatment options targeting metabolic pathways including GLUT1 inhibitors may offer a promising therapeutic modality in glandular diseases and cancers.

Keywords: Sublingual salivary gland, GLUT1, striated ducts, female rats

1. Introduction

Salivary glands are exocrine, merocrine, compound, tubulo-alveolar glands that are specialized for formation and secretion of saliva. According to size, salivary glands are classified into major and minor glands (Nanci, 2018).

The sublingual salivary glands (SLGs) are major salivary glands that produces mixed fluid rich in mucins and accounts for 5% of the daily salivary secretion. It is formed of stromal and parenchymal

components. The parenchymal part includes the acini, duct system and the myoepithelial cells. The acini forming cells are the cells producing the primary saliva and drain their secretion into the duct system. The duct system started with smaller intercalated ducts which are not well developed in SLGs (Nanci, 2018). These smaller ducts drain into longer and larger striated ducts (SDs), and thereafter to the excretory ducts. The SDs are lined by columnar cells with central, spherical nuclei and acidophilic cytoplasm. The SD possessed polarized cells with short microvilli at their luminal surface. Abasement membrane separates the basal surface from the surrounding connective tissue. The basal part reveals basal folding of the basal plasma membrane. In between these folds, mitochondria are loaded giving the duct a striated appearance. These folds provide large surface area for active transport and the energy requirements are provided by the mitochondria. The electrolyte reabsorption takes place in the SD with reabsorption of chloride and sodium and secretion of bicarbonate and potassium against the concentration gradient and without loss of water. Therefore, the salivary secretion changed from isotonic to hypotonic fluid. The mucous secretion of the acini is modified in the SDs as they play significant role in ions' active transport, which leads to the change of saliva from isotonic to hypotonic in nature (Berkovitz et al., 2018; Nanci, 2018).

Glucose transporters (GLUTs) are a large family of proteins that allow glucose transport. Fourteen members of GLUTs have been identified (Ismail and Tanasova, 2022; Peng and Zeng, 2024). These transporters have specific distribution in the body tissues. There is a different affinity of GLUTs to glucose and the GLUTs family is subdivided into 3 classes. The class I of GLUTs are (GLUT1, 2, 3, 4 and 14) and are responsible for the membrane pass of glucose and other hexoses excluding fructose. The class II of GLUTs includes (GLUT 5, 7, 9 and 11) and this class is responsible for the transport of fructose. The class III of GLUTs involves (GLUT6, 8, 10, 12, and 13) and these members possess an atypical structure (Ismail and Tanasova, 2022)

One of the most widely studied GLUTs and is ubiquitously distributed in the body tissues is GLUT1 (Ismail and Tanasova, 2022; Pragallapati and Manyam, 2019; Peng and Zeng, 2024). GLUT1 is highly upregulated during embryonic period of development thereafter is progressively decreased in gestation. It is expressed in the brain, erythrocyte membrane, eyes, kidney, peripheral nerves, colon and placenta. In addition, GLUT1 has a pivotal role in maintaining angiogenesis and endothelial functions (Peng and Zeng, 2024).

The GLUT1 displays distinct expression and distribution patterns in the rodent submandibular tissues. The duct system of the submandibular glands revealed strong immunohistochemical staining in the basolateral membrane, however weak staining was detected in the secretory units in rat and mouse submandibular glands (Cetik et al., 2014). GLUT1 has been detected in the parotid gland acini, in both the basolateral and apical membranes. It has been suggested that GLUT1 in the parotid glands plays a role in transporting glucose to the acinar lumen (Jurysta et al., 2012). Interestingly, GLUT1 is expressed at a high level in the pleomorphic adenoma and the carcinoma ex pleomorphic adenoma (Scarini et al., 2020).

Although the localization of GLUT1 in the parotid (Jurysta et al., 2012) and submandibular (Cetik et al., 2014) glands has been reported, the distribution patterns of GLUT1 in the SLGs is hitherto unknown. Therefore, this study was designed to assess GLUT1 localization in the SLG's acini and SDs and the comparative optical intensity of the GLUT1 immunoreaction in the SLG's acini and SDs in female control rats.

2. Materials and Methods

2.1. Ethical Statement

This study experimental procedures were granted the ethical approval from the Scientific Research Ethics Committee at the Faculty of Dentistry, Minia University in Egypt (committee No: 108, Decision No: 938). The study procedures were performed in agreement with the national ethical and ARRIVE guidelines and with the National research council's guide for care and use of experimental animals (Percie du Sert et al., 2020; Council, 2011).

2.2. The Experimental Design

The sample size was established on the basis of a published study (El-Badawy et al., 2024). The sample size and Post-hoc power were determined utilizing power analysis and sample size software (PASS 2020, NCSS, LLC, Kaysville, Utah, USA). The minimal sample size was estimated to be seven rats per group with an effect size of 10%, power 80% and level of significance 5% utilizing Chi square test (Grimes and Schulz, 1996; Kim et al., 2022). Eight adult healthy female albino rats were utilized and weighed (200-250 g). The animals were maintained in the animal housing, at Assiut University-Faculty of Veterinary Medicine, in wire mesh cages with a temperature of $25 \pm 1^\circ\text{C}$, humidity of $30 \pm 35\%$ and a light-controlled room. Diet and water were given ad libitum.

All rats were euthanized by an overdosage of sodium pentobarbital 40 mg/kg, IP and thereafter by cervical dislocation. The SLGs were carefully dissected bilaterally, and the glandular tissues were fixed in 10% formalin for 48 h (El-Badawy et al., 2024).

2.3. Sample preparation and sectioning

The SLG samples were rinsed in Phosphate buffered saline (PBS) and kept in 70% ethanol overnight at 4°C . Thereafter, the tissue samples were dehydrated in (70%, 95%, 99.5%) ethanol (3 baths, 30 minutes per bath) and cleared in xylene (5 baths, 5 minutes per bath). Then the samples were infiltrated by several changes of wax (5-6 baths, 20 minutes per bath), followed by embedding in paraffin and fixing the bases. After sectioning the wax blocks into $6\ \mu\text{m}$ thick sections, the tissue ribbons were mounted on the glass slides (StarFrost, Kitteglass, Germany) (El-Badawy et al., 2024).

2.4. The H&E staining

The H&E staining was performed to show the general histological structure of the SLGs. The tissue sections were deparaffinized in xylene, rehydrated in alcohol (99.5%, 95% and 70%) and washed in distilled H₂O. Thereafter, the sections were stained in hematoxylin for 3 minutes and washed under tap H₂O up to 20 minutes. The sections were stained for 2 minutes in eosin Y (Cardiff et al., 2014) and thereafter, dehydrated in alcohol. Thereafter, the sections were exposed to 2 bathes of xylene followed by mounting and cover-slipping (El-Badawy et al., 2024).

2.5. Masson trichrome staining

Masson trichrome staining was performed to show the collagen fiber distribution in the SLGs. The SLG tissue sections were dewaxed in xylene, followed by rehydration in ethanol. The sections were rinsed in deionized water and were stained with Erlich's hematoxylin followed by incubation with fuschien in glacial acetic acid. After incubation with molybdenum phosphoric acid, the tissue sections were processed for mounting (Pringle et al., 2016).

2.6. The GLUT1 Immunohistochemistry

To evaluate the localization of GLUT1 in the SLG tissue, the GLUT1 protein was assessed by immunohistochemistry. After deparaffinization and rehydration, the tissue sections were washed in PBS and antigen retrieved in citrate buffer (10 mM) (pH 6) in the microwave (10 minutes) at high power to unmask the target antigens. The SLG tissues were allowed to cool down followed by rinsing in distilled H₂O at room temperature. Thereafter, the tissue sections were exposed to 3% H₂O₂ for 20 minutes to block the endogenous peroxidases. After incubation with anti-GLUT1 (1:50, MA5-31960, Thermo Fisher), the sections were washed in PBS followed by incubation with secondary antibody (EnVision FLEX/HRP, DAKO, Denmark). This was followed by rinsing in baths of PBS. After developing for 10 minutes in diaminobenzidine (DAB+chromogen, EnVision FLEX, DAKO, Denmark), the tissue sections underwent counterstaining in Mayer's hematoxylin and mounting (El Badawy et al., 2024; Júnior et al., 2016).

2.7. Histomorphometry

The GLUT1 immunoreaction optical intensity was analyzed utilizing Image J (NIH, USA, version 1.48 v) software. The measurements were done utilizing a standard measuring frame, using five non-overlapping

fields were utilized for each sample (n=8) at x400 magnification, and the mean value of each specimen was calculated (El Badawy et al., 2024).

2.8. Statistics

The data were analyzed utilizing Paired t-test, in order to compare the GLUT1 immunoreaction optical intensity between the mucous acini and the SDs of the SLGs. The data were shown as mean \pm standard deviation and p-value below 0.05 designates significant difference. The analysis was performed utilizing IBM SPSS software v. 20.0 (ARMONK, NY: IBM Corp).

3. Results

3.1. Histology of the SLG acini and striated ducts

The SLG structure in the control rats, depicts mucous acini which are tubular in form. The acini consist of pyramidal shaped mucous cells with broad base, narrow apex and surrounding central lumen. The nuclei are flattened and basal in position. The apical portion of the cells is loaded with poorly stained secretory granules of mucous type (Fig. 1, 2). The SDs are the principal duct in the gland lobules and consist of columnar cells with a nucleus which is central in position. In addition, the SDs reveal basal striations. In addition, small secretory granules are situated in the apical part of the duct. The ductal lumen is wider than that of the acini (Fig. 1, 2). Fine collagen fibers partition the glands into lobules (Fig. 2A, B).

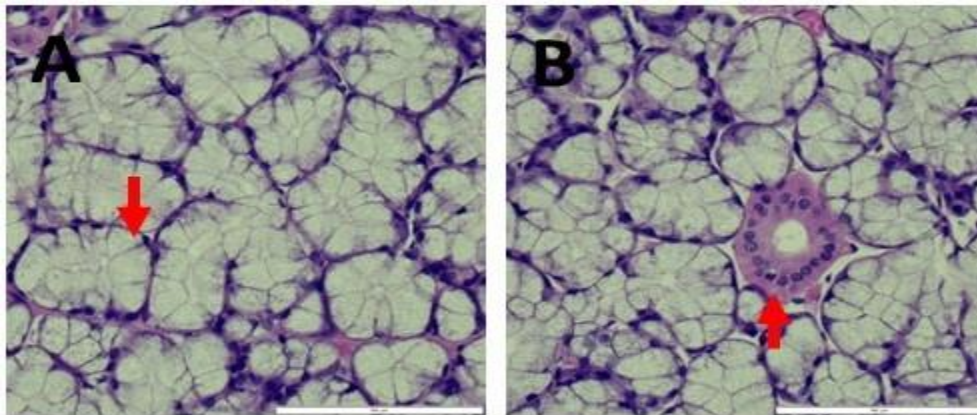


Figure 1. Histology of adult sublingual salivary gland (SLG) of control female rats. A and B are SLG images stained with hematoxylin and eosin of control rats. (A) The SLG of controls displays mucous acini with flattened basal nuclei (red arrow). (B) The striated ducts reveal central nuclei and basal striations (red arrow). Scale bar: 50 μ m

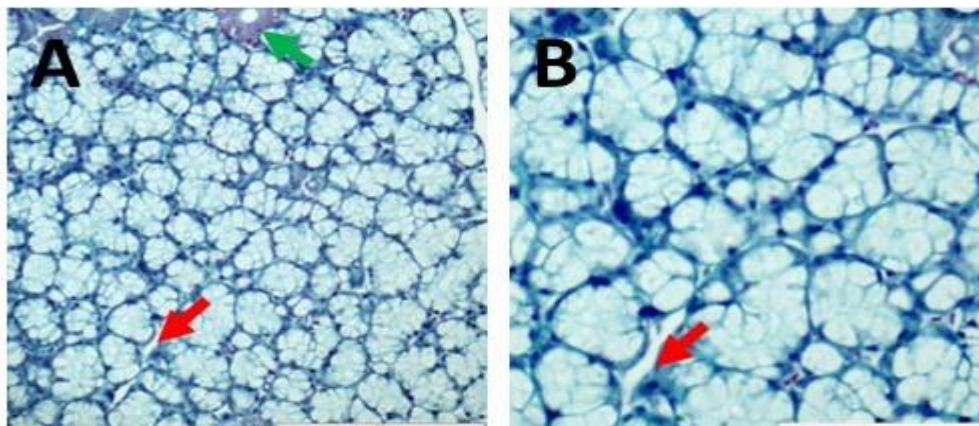


Figure 2. Adult sublingual salivary gland (SLG) of control female rats stained with Masson trichrome. (A and B) the SLG of controls displays mucous acini with fine connective tissue fiber separating between the SLG's lobules (red arrow). The striated ducts reveal central nuclei and basal striations (green arrow). Scale bar: (A,) 100 μ m; (B) 50 μ m

3.2. Immunolocalization of GLUT1 in the SLG acini and the SD

In the control rats, GLUT1 was detected in the SLG acini and in the SD. The SLG acini depicted an apparently moderate GLUT1 immunolabelling occupying the thin basal rim of the mucous acini cytoplasm (Fig. 3A). The SD of the SLGs revealed an apparently strong GLUT1 immunoreaction in the cytoplasm of the SD masking the SD nuclei (Fig. 3B).

Histomorphometric analysis of GLUT1 immunoreaction optical intensity revealed statistically significant increase of GLUT1 immunolabelling intensity in SDs in comparison to the mucous acini in the SLGs (P=0.000) (Table 1) (Fig. 3C).

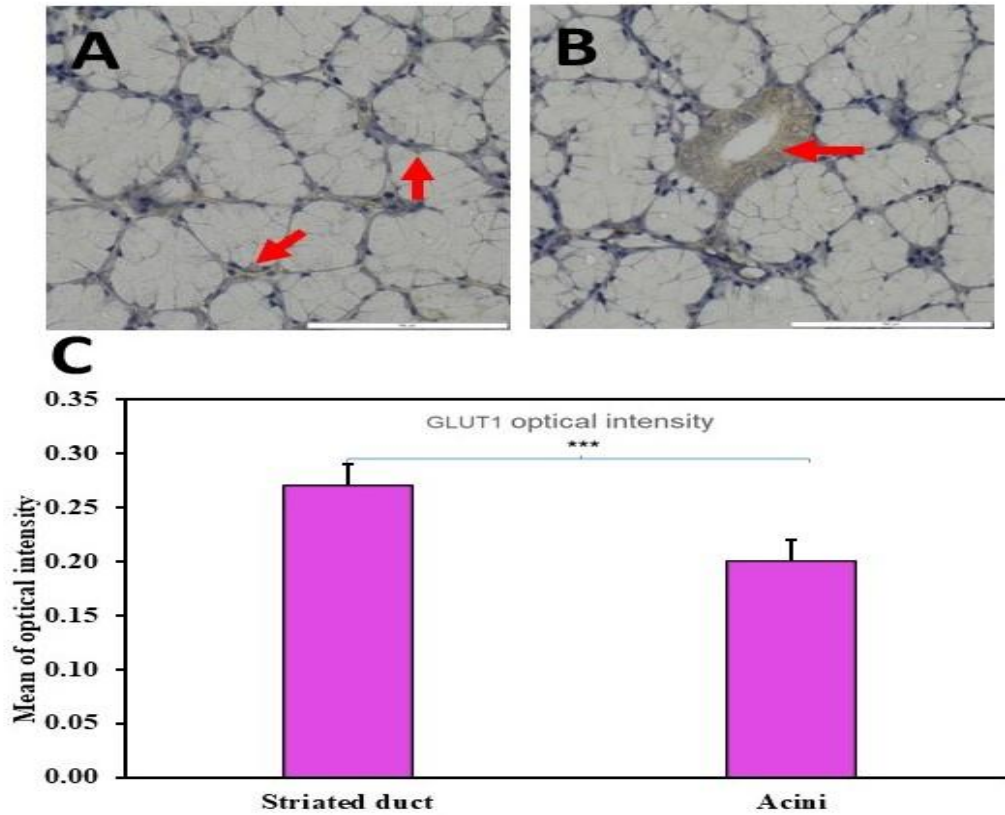


Figure 3. GLUT1 localization in the adult sublingual salivary gland (SLG) of female control rats. (A, B) are representative GLUT1 immunostained section images of SLGs of control rats. (A) The SLG controls display moderate GLUT1 immunolabelling in the mucous acini (red arrows). (B) The striated ducts (SDs) reveal strong GLUT1 immunoreaction (red arrows). Scale bar: (A, B) 50 μ m. (C) bar graph representing higher optical intensity of GLUT1 immunoreaction of the SDs in comparison to the acini in the SLGs, data are presented and analyzed by Paired t-test, n=8, and p< 0.001.

Table 1: Comparison between the GLUT1 optical intensity in the SLG acini and SDs

The GLUT1 immunoreaction Optical intensity	Striated duct (SD)	Acini	t	p
Mean \pm SD.	0.27 \pm 0.02	0.20 \pm 0.02	8.83*	<0.001*

5. Conclusion

The present study revealed moderate GLUT1 immunoreaction in the SLG acini and strong immunolabelling in the SDs. Localization of GLUT1 in the acini of the SLGs suggests role of GLUT1 in glucose delivering for the energy needs of the acini for protein synthesis and for the process of exocytosis. In addition, the localization of GLUT1 in the SDs suggests role in securing the high energy demands by the SDs for ions' reabsorption. Identification of the GLUT1 in normal tissues of the SLG is of clinical importance, as it provides insights in the diagnosis and treatment of the SLG disorders

6. Acknowledgements

Abbreviations

GLUT1	Glucose transporter 1
GLUTs	Glucose transporters
H&E	Hematoxylin and eosin
PBS	Phosphate buffered saline
SDs	Striated ducts
SLGs	Sublingual salivary glands

CRedit authorship contribution statement

Maha El Shahawy^{1,2,*}: Conceptualization, Data curation, Formal analysis, investigation, methodology, Resources, Supervision, Validation, Visualization, Writing - original draft, writing-review and editing

Menna Abdulqader El-Badawy³: Funding acquisition; Investigation; Methodology; Resources, Validation; Visualization; Writing - review and editing.

All authors have read and agreed to the published version of the manuscript.

Declaration of competing interest

None

Funding

This research did not receive any specific grant from funding agencies in the public, commercial or not-for-profit sectors.

References Cited

- Baer S.C., Casaubon L., Younes M. Expression of the human erythrocyte glucose transporter Glut1 in cutaneous neoplasia. *J. Am. Acad. Dermatol.* 1997;37:575–577.
- Berkovitz BKB, Holland GR, Moxham BJ. (2018). *Oral Anatomy, Histology and Embryology* (5th Ed)
- Buchwalow, I. B., & Böcker, W. (2010). *Immunohistochemistry: Basics and Methods* (pp. 31–39).
- Cardiff, R. D., Miller, C. H., & Munn, R. J. (2014). Manual hematoxylin and eosin staining of mouse tissue sections. *Cold Spring Harbor Protocols*, 2014(6), 655–658.
- Cetik, S., Hupkens, E., Malaisse, W. J., Sener, A., & Popescu, I. R. (2014). Expression and Localization of Glucose Transporters in Rodent Submandibular Salivary Glands. *Cellular Physiology and Biochemistry*, 33(4), 1149–1161.
- Chen Z, Dudek J, Maack C, Hofmann U. Pharmacological inhibition of GLUT1 as a new immunotherapeutic approach after myocardial infarction. *Biochem Pharmacol.* 2021 Aug;190:114597
- Cibrian D, de la Fuente H, Sánchez-Madrid F. Metabolic Pathways That Control Skin Homeostasis and Inflammation. *Trends Mol Med.* 2020 Nov;26(11):975-986
- Council, N. R. (2011). *Guide for the Care and Use of Laboratory Animals* (8th ed.). National Academies Press.
- El-Badawy MA, Badawy M, El Shahawy M. Bone marrow derived mesenchymal stem cells restored GLUT1 expression in the submandibular salivary glands of ovariectomized rats. *Arch Oral Biol.* 2024 Oct;166:106048.
- Grimes, D., & Schulz, K. (1996). Determining Sample Size and Power in Clinical Trials: The Forgotten Essential. *Seminars in Reproductive Medicine*, 14(02), 125- 131. <https://doi.org/10.1055/s-2007-1016320>

- Heydarzadeh S, Moshtaghie AA, Daneshpoor M, Hedayati M. Regulators of glucose uptake in thyroid cancer cell lines. *Cell Commun Signal*. 2020 Jun 3;18(1):83.
- Ismail, A., & Tanasova, M. (2022). Importance of GLUT Transporters in Disease Diagnosis and Treatment. *International Journal of Molecular Sciences*, 23(15), 8698.
- Jurysta, C., Nicaise, C., Cetik, S., Louchami, K., Malaisse, W. J., & Sener, A. (2012). Glucose Transport by Acinar Cells in Rat Parotid Glands. *Cellular Physiology and Biochemistry*, 29(3–4), 325–330.
- Jurysta, C., Nicaise, C., Giroix, M.-H., Cetik, S., Malaisse, W. J., & Sener, A. (2013). Comparison of GLUT1, GLUT2, GLUT4 and SGLT1 mRNA Expression in the Salivary Glands and Six Other Organs of Control, Streptozotocin-Induced and Goto-Kakizaki Diabetic Rats. *Cellular Physiology and Biochemistry*, 31(1), 37–43.
- Júnior, A. M., de Amorim Carvalho, F. A., de Oliveira Dantas, W., Gomes, L. C., da Silva, A. B., de Sousa Cavalcante, M. M., de Oliveira, I. M., de Deus Moura de Lima, M., Rizzo, M. dos S., de Carvalho Leite, C. M., Moura, S. M. dos S., de Deus Moura, L. de F. A., & da Silva, B. B. (2016). Does Leishmaniasis disease alter the parenchyma and protein expression in salivary glands? *Experimental Biology and Medicine*, 241(4), 359–366.
- Kamata M, Shirakawa M, Kikuchi K, Matsuoka T, Aiyama S. Histological analysis of the sublingual gland in rats with streptozotocin-induced diabetes. *Okajimas Folia Anat Jpn*. 2007 Aug;84(2):71-6.
- Kim, J. M., Kim, J. H., Kim, K., Shin, S. C., Cheon, Y. I., Kim, H. S., Lee, J. C., Sung, E.S., Lee, M., Park, G. C., & Lee, B. J. (2022). Tonsil mesenchymal stem cells-derived extracellular vesicles prevent submandibular gland dysfunction in ovariectomized rats. *Aging*, 14(5), 2194–2209.
- Maruo, K., Nishiyama, M., Honda, Y., Cao, A.-L., Gao, W.-Q., Shibata, K., Murata, Y., & Kido, M. A. (2023). Increased GLUT1 expression and localization to Golgi apparatus of acinar cells in the parotid gland of Goto-Kakizaki diabetic rats. *Archives of Oral Biology*, 146, 105601.
- Nanci, A. (2018). Salivary Glands. In Ten Cate's Oral Histology; Development, Structure, and Function (9th ed.).
- Peng Q, Zeng W. The protective role of endothelial GLUT1 in ischemic stroke. *Brain Behav*. 2024 May;14(5):e3536.
- Percie du Sert, N., Hurst, V., Ahluwalia, A., Alam, S., Avey, M. T., Baker, M., Browne, W. J., Clark, A., Cuthill, I. C., Dirnagl, U., Emerson, M., Garner, P., Holgate, S. T., Howells, D. W., Karp, N. A., Lazic, S. E., Lidster, K., MacCallum, C. J., Macleod, M., Pearl, E. J., Petersen, O. H., Rawle, F., Reynolds, P., Rooney, K., Sena, E. S., Silberberg, S. D., Steckler, T., & Würbel, H. (2020). The ARRIVE guidelines 2.0: Updated guidelines for reporting animal research. *Br J Pharmacol*, 177(16), 3617–3624.
- Pragallapati, S., & Manyam, R. (2019). Glucose transporter 1 in health and disease. *Journal of Oral and Maxillofacial Pathology: JOMFP*, 23(3), 443–449.
- Pringle S, Maimets M, van der Zwaag M, Stokman MA, van Gosliga D, Zwart E, Witjes MJ, de Haan G, van Os R, Coppes RP. Human Salivary Gland Stem Cells Functionally Restore Radiation Damaged Salivary Glands. *Stem Cells*. 2016 Mar;34(3):640-52.
- Scarini JF, Rosa LF, Souza RAL, Egal ESA, Tincani AJ, Martins AS, Kowalski LP, Graner E, Coletta RD, Carlos R, Gondak RO, de Almeida OP, Altemani AMAM, Bastos DC, Mariano FV. Gene and immunohistochemical expression of HIF-1 α , GLUT-1, FASN, and adipophilin in carcinoma ex pleomorphic adenoma development. *Oral Dis*. 2020 Sep;26(6):1190-1199.
- Vrhovac Madunić I, Karin-Kujundžić V, Madunić J, Šola IM, Šerman L. Endometrial Glucose Transporters in Health and Disease. *Front Cell Dev Biol*. 2021 Sep 6;9:703671.
- Xu JQ, Fu YL, Zhang J, Zhang KY, Ma J, Tang JY, Zhang ZW, Zhou ZY. Targeting glycolysis in non-small cell lung cancer: Promises and challenges. *Front Pharmacol*. 2022 Nov 30;13:1037341.